Supporting Information for "A Geochemical Review of Amphibolite, Granulite, and Eclogite Facies Lithologies: Perspectives on the Deep Continental Crust"

Laura G. Sammon[1], William F. McDonough[1,2]

[1]Department of Geology, University of Maryland, College Park, MD 20742, USA

[2]Department of Earth Sciences and Research Center for Neutrino Science, Tohoku University, Sendai 980-8578, Japan

Contents of this file

1. Multi-modality in Oxides, Further Discussion
2. Eu anomalies
3. Various elemental trends
4. Figures S1 to S2, sample locations
5. Figures S3 to S9, additional major and trace element data

Additional Supporting Information (Files uploaded separately)

1. Geochemical datasets (totals outside of 100 $\pm$ 10 % not included)
2. Pb isotope and $\kappa_P b$ data
3. Extended tables for minor and trace elements, various element ratios, and κ_{Pb}

1. Multi-modality in Oxides, Further Discussion

Many major oxides show biasing towards either mafic or felsic compositions. This means that the predictors of the oxide's central value is neither mafic or felsic, but a mixture of two or more modes from the ensemble data. One of many tests for unimodality or multimodality in a distribution is the Hartigan's Dip Test (Hartigan & Hartigan, 1985). We applied this statistical test to our datasets in an attempt to quantify the presence of multimodal trends, namely the Daly Gap. Table ST13 lists the results. Oxides with values closer to 1 are more likely to have a unimodal distribution. A challenge we find is in determining where to put the cutoff for unimodal vs. bimodal (multimodal) distribution. For example, SiO_2 has Dip Test value that reflects its bimodality. In other datasets, however, such as FeO_T, the gap is less clear. Visual assessments of bimodality in the dataset are heavily influenced by the binning of data (e.g. Fig. S3) and lead to ambiguous results. Each dataset was randomly sampled 10,000 times to minimize differences in results solely because one set had more data points than another.

FeO_T and MnO appear to be bimodal in all of the granulite facies lithologies, including granulite facies xenoliths. Their Dip Test values are likely affected by the discontinuous pattern of FeO_T abundances and a few outliers in MnO concentrations. While Post Archean granulite facies terrains do likely show evidence of the Daly Gap in their FeO_T distributions, it is once again difficult to say conclusively whether bimodality is actually evident in Archean granulite facies terrains' FeO_T. MnO is once again plagued by outliers both in granulite and amphibolite facies lithologies.

K_2O content is highly variable, spanning at least six orders of magnitude for each dataset. K_2O distributions in granulite and eclogite facies xenoliths approach log-normal, but granulite facies terrains and amphibolites are skewed towards low K_2O values. The abundance of K_2O depends on the crystallization of K-feldspars (Rudnick & Presper, 1990). If K-feldspar is present, K behaves like a major element. If K-feldspar does not crystallize, K behaves like a trace element.

Multimodality in the other oxides is also open to debate. MgO stands out as potentially bimodal in amphibolite facies lithologies but is heavily influenced by the number of data bins. When the number of bins is increased, we see a secondary peak developing towards low MgO concentrations (Figure S3). We run into the same trouble when looking at Na_2O and CaO; whether or not they appear bimodal depends on the data binning. CaO seems to be the most likely candidate for multi-modality when binned according to Sturge's Law but becomes more unimodal as the number of bins increases. All Dip Test values for eclogite facies lithologies are elevated compared to amphibolite and granulite facies lithologies because of eclogite's fewer numbers and increased variability.

2. Eu Anomalies

All amphibolite, granulite, and eclogite facies lithologies have similar median Eu anomalies ($\frac{Eu}{\sqrt{Sm_N * Gd_N}}$). While granulite facies lithologies tend to show more variation in Eu anomalies (Figure S4), the median Eu/Eu* values for all of our groups fall between 0.89 and 1.2. The distributions of Eu/Eu*, shown in Figure S4, are skewed towards the right, moreso for granulite facies than for other facies, favoring Eu/Eu* values around 1 but reaching as high as 2-3. These values of Eu/Eu* < 1 (which translate to negative median Eu anomalies) are in line with previous estimates for the middle and lower crust

and could indicate voluminous crustal recycling (Tang et al., 2017). The lack of strong, positive Eu anomalies in the deep crust counters the argument that the deep (or lower) crust is complementary to the upper crust, which also has a negative Eu anomaly (Taylor & McLennan, 1985).

3. Element Trends

3.1. Fluid Mobile Elements

3.1.1. K, Rb, and Cs

The transition from amphibolite to granulite facies can be considered, for the major elements, an isochemical dehydration reaction, but this is not the case for the most fluid mobile elements: K, Rb, and Cs. Consistent with the observations of (Rudnick & Presper, 1990), K_2O/Rb ratios in amphibolite and granulite facies lithologies are negatively correlated with K_2O content, especially at K_2O <1.2 wt.%, indicating Rb depletion relative to K_2O. We restrict our analysis of K_2O/Rb to compositions to rock with > 55 wt.% SiO_2 because the K_2O/Rb ratios of unmetamorphosed basalts are highly variable, making it difficult to evaluate Rb depletion in mafic lithologies (Rudnick & Presper, 1990). K_2O/Rb ratios reach a maximum at about 1 in most of the metamorphic datasets. Although we omit them, mafic lithologies follow the same trend, though lower K_2O values are reached. As suggested by various studies, this trend likely reflects a mineralogical control on the partitioning of Rb and K between minerals and a fluid phase (e.g., Rudnick et al., 1985; Fowler, 1986). Low concentrations of K_2O and Rb, and high K_2O/Rb ratios, may reflect igneous processes rather than metamorphic processes (Van Calsteren et al., 1986). However, several mafic granulite facies and amphibolite facies lithologies have high K/Rb ratios compared to basalts, which suggests that they have experienced some Rb depletion

during metamorphism (Stosch et al., 1986; Rudnick & Taylor, 1987). The similarities between the amphibolite and granulite facies K/Rb are striking, because high K_2O/Rb was thought to be the providence of dehydration metamorphism. Partial dehydration of amphibolite facies lithologies might lead to high K_2O/Rb ratios while still leaving behind enough hydrous mineral assemblages to classify the rock as amphibolite. Future studies should explore the quantification of dehydration as it relates to K_2O/Rb ratios. Alternatively, metamorphosing gabbro to the amphibolite facies can produce uneven increases in K and Rb (Field & Elliott, 1974), leading to lower K_2O/Rb ratios. Low K_2O/Rb ratios in amphibolites could also be inherited from the retrograde metamorphism of granulite with low K_2O/Rb (Field & Clough, 1976).

3.1.2. La/Th and Th/U

Granulite facies lithologies and eclogite facies terrains show greater Th and U depletion than amphibolite facies lithologies or eclogite facies xenoliths. While the granulite and amphibolite facies lithologies show comparable amounts of U loss, indicated by elevated Th/U and low La/Th values, the granulite facies lithologies can reach almost an order of magnitude greater La/Th values with low Th/U, indicating a loss of both U and Th. U can be depleted through loss of water due to its redox sensitivity (U^{6+} is fluid mobile; U^{4+} is not), though both U and Th depletions typically indicate a lack of U and Th-bearing accessory phases (Rudnick et al., 1985; Fowler, 1986). Archean granulite facies terrains reach higher levels of U depletion than Post-Archean terrains, a curious observation since many Archean terrains contain monazite, a Th and U-bearing accessory phase (Rudnick & Presper, 1990). Eclogite facies lithologies on the whole have Th/U ratios around 2 and a wider range (0.1 to 20) in La/Th.

3.1.3. Alkalis and Alkaline Earth Metals, in General

The alkali and alkaline earth metals are, generally, large ion lithophiles due to their low charges and high ionic radii. The abundance of these fluid mobile elements becomes more variable as ionic radius increases, with Rb and Cs having the greatest variability and greatest fluid mobility. Samples that lack K-feldspar typically display depletions in K, Rb, and Cs while Na and Ca remain rather remarkably invariable outside of their felsic and mafic modes. Ba is also quite variable with relative uncertainties ranging from 100 to 200% (similar to Rb, Cs, and La, though Ba is more normally distributed than those three). Many of the amphibolite and granulite facies lithologies are also metaluminous, though our samples span the range of peraluminous to peralkaline.

As alluded to in Section 3.1.3, the alkali metals show considerable variability. K, Rb, and Cs increase in skewness as their ionic radius increases, with Cs being the largest and most labile. Rb is also incompatible and fluid mobile. We suspect much of the variation in K stems from the presence or absence of K-feldspar. Lithium also shows a moderate to high level of variability in amphibolite and granulite facies, which could be the result of Li's fluid mobility. Ba and Sr, also incompatible and fluid mobile elements, vary more than their smaller radii counterparts, Mg and Ca, but not nearly as much as the alkalis.

3.2. High Field-Strength Elements

Eclogite facies lithologies display the most fractionation of the generally insoluble high field strength elements (HFSEs). Of the HFSEs, Ta and Mo display the largest spread and highest uncertainties for most of our lithologies. There is not enough data to plot Mo or Ta for eclogite facies lithologies. Once more Mo data are reported, paired spikes in both Mo and Nb content in eclogites could indicate that Mo and Nb, which have

similar ionic radii, are both being retained in rutile (Rudnick et al., 2000). With 64 data points, granulite facies xenoliths' elevated Mo is more of a conundrum. High abundances of rutile are not expected for granulite facies xenoliths (Rudnick & Presper, 1990), and the xenoliths do not have a complementary Nb spike. Since titanite (sphene), ilmenite, and magnetite typically host the greatest abundance of Mo in crustal rocks (Greaney et al., 2018), along with rutile, it is possible that these minerals exist in higher abundances in granulite facies xenoliths and/or the deep crust than previously thought.

The data also show variable depletions in Ta compared to (Rudnick & Gao, 2014)'s value. Nb/Ta values also exceed previous lower crustal estimates (Rudnick & Gao, 2014), mimicking more the middle crust's ratio, suggesting that the deep crust might have a super-chondritic Nb/Ta ratio. Plotting Nb vs. Ta (Figure S8) yields a linear log-log plot for amphibolite, granulite, and eclogite facies lithologies. In many cases, we do not have high resolution measurements for Ta concentrations at the sub-ppm level, evidenced by the diagonal lines of data on the Nb vs. Nb/Ta plots (ratios dominated solely by changing Nb) and horizontal array of dots on the Ta vs. Nb/Ta plots. Concentrations which have been rounded to the nearest 100 ppb or ppm when reported. Eclogite facies xenoliths and terrains have notably different Nb/Ta ratios: 15.6 ± 1.9 and 22.4 ± 10.2, respectively. Studies have hypothesized that Nb can be sequestered by rutile in eclogite formation, but Ta is not expected to increase (Rudnick et al., 2000). Eclogitic material in down-going crustal slabs could be a complementary reservoir to the apparent Nb depletion in the rest of the observable bulk silicate Earth.

3.3. Transition Metals

Transition metal data exists in more abundance for amphibolite facies lithologies than for granulite or eclogite. Trends in the first row transition elements are discussed in depth in Section 6 of the main text, but we wanted to briefly mention them in context with the other elements here. The dearth of data on moderately and highly siderophile elements is because they exist in such low abundances in the silicate portion of Earth that only recently have we been able to obtain high precision measurements.

Ti, Zr, and Hf have similar variability, with more mafic lithologies having lower absolute concentrations of Zr. Eclogite facies lithologies have the lowest concentrations of all three elements, a curious finding considering that eclogite facies lithologies tend to have an abundance of rutile ($FeTiO_2$). Though they track similarly, what controls the abundance of Ti family elements is unclear.

The Cr family, on the other hand, shows much greater variability, perhaps due to Cr concentrating in garnets, spinels, chromite, or even olivine. Olivine fractionation in the source melt could also explain the variations also seen in Ni (Arndt, 1994) among amphibolite and granulite facies lithologies. However, Mo's slightly chalcophile behavior (e.g., Barnes, 2016) could be lending the Cr-family a more discontinuous and variable look than, for example, the Sc, Ti, or Mn families. The Ni and Cu display more variable abundances as well, especially in amphibolite facies lithologies. Their behavior could be attributed to S-affinity and/or the presence of Ni- or Cu-bearing accessory mineral phases (e.g., olivine, dioptase). Weathering has been shown to (e.g., Arndt, 1994; Polat et al., 2002), making it more likely that the spread of Cr and Ni abundances is controlled by igneous factors.

A stepped increase in variability is visible from the top to the bottom of the V family for both amphibolite and granulite facies lithologies. This trend, notable in other parts of the periodic table is discussed in Section 6 of the main text. Of course, limited sample numbers may be causing the fluctuation in third-row transition metal abundances. More data is always welcomed to better constrain the abundances and behaviors of the transition metals.

Not much can be said about the elements towards the bottom and right of the periodic table for granulite facies lithologies due to a lack of data, though we can devise a few hypotheses to explain the increased spread in abundances of heavier elements compared to their lighter counterparts. Especially in heavy elements that do not lack for data, such as Ta, Pb, Th, and U, the continuous but wide distribution of data could be caused by the vertical fractionation of these elements within the continental crust. Vertical fractionation of elements within the crust has been discussed in depth for decades (e.g., Sighinolfi, 1971; Taylor & McLennan, 1985; Rudnick & Gao, 2014). One means for testing this hypothesis is comparing trace element abundance to inferred maximum pressure conditions - the higher the pressure, the deeper from within the crust the sample originated. Sadly, most of our data does not have precise pressures and/or temperatures associated with it, though some studies have explored these composition-pressure relationships with quantitative methods (e.g., Bohlen & Mezger, 1989; Rudnick & Jackson, 1995; Barnhart et al., 2012).

Cr, Ni, and Cu break the homogeneity of the first row transition elements. Cr and the two other elements it shares a family with, Mo and W, are more variable than any other transition metals, though we must consider that Mo and W have fewer analyses than many of the others (89 and 42 data points, respectively, compared to the 1000's of analyses

done on first row transition elements and Y, Zr, Nb, Hf, and Ta). The Cr family takes on an abnormal valence electron structure ($4s^1 3d^5$). This causes Cr to have a range of valence states, though it commonly exists in a 3+ valence state as a substitution in garnet (uvarovite, $Ca_3Cr_2(SiO_4)_3$). Mo and W are high field strength elements with high valences and large radii, which make it harder for them to substitute into common minerals and may contribute to their variability. Mo is typically hosted in Ti-oxides though displays much more variation than Ti.

The Ni and Cu families might also be special cases, not because of their valence structure, but because of their metal and sulfide affinity. The variability in S content may cause fluctuations chalcophile-siderophile elements (CSEs), including Ni and Cu. Of the other CSE's, Zn, a moderately chalcophile element (Jenner, 2017), is much more normally distributed than either Ni or Cu. There are too few measurements on Au and Ag to determine whether their apparent variation is caused by CSE (Jenner, 2017) behavior or if they are under-sampled. The Cu and Ni distributions have far more outliers than any other first row transition metals. Cross-referencing the original data sources show that $>$ 1100 amphibolite and $>$ 900 granulite measurements come from samples with 0.01 - 0.1 wt.% Cu or Ni. The spread in Cu and Ni compositions could be due to cumulate formation and recycling processes, whereby CSE's can be partitioned by magnetite-induced sulfide fractionation in lower crustal settings. While we expect enrichment in CSE's in these lower crustal cumulates, delamination of such material could also cause depletion and contribute to the bulk crust's low Cu concentrations.

3.4. Halogens

Limited data is available for the halogens in these medium and high grade metamorphic lithology datasets. F and Cl are the only elements measured for amphibolite and granulite facies lithologies. No halide data is available for eclogite facies lithologies in our dataset. Halides can be transported in fluids or incorporated into select mineral phases, such as Cl-rich biotite and amphibole, apatite, and fluorite (Kusebauch et al., 2015). High solubility in water means these elements are often mobilized by fluid fluxing and can often be found as chemical weathering and alteration byproducts in granulites, despite granulites being nominally anhydrous (e.g., Markl et al., 1997; Banks et al., 2000; Kusebauch et al., 2015). Stable Cl isotopes have been studied in granulites to track mantle participation in silicate Earth's Cl cycle and fluid infiltration processes (Markl et al., 1997). However, the volatility of halogens and their incompatibility in many melt systems has resulted in relatively low halide abundances in the deep crust outside of fluid processes.

4. Supplementary Tables

Table S1: Amphibolite Facies Lithologies

	Mean	Median	Geometric Mean	γ Mean	STD	IQR	Geo STD	γ STD	N (filtered)	N (original)
Li	17.9	15.0	14.8	17.9	10.7	14.5	1.89	10.6	455	727
Be	1.57	1.44	1.21	1.57	1.02	1.10	2.22	1.08	212	374
B	14.0	9.00	8.44	14.0	14.5	15.6	2.81	13.1	184	362
N	-	-	-	-	-	-	-	-	0	0
F	435	399	60	435	351	512	48.2	746	180	269
S	41.2	22.0	25.2	41.2	46.1	44.0	2.6	38.2	93	292
Cl	51.0	29.3	1.2	51.0	62.2	86.7	83.3	114	81	196
Sc	23.1	21.0	18.3	23.1	13.6	24.4	2.11	15.2	1360	3160
V	152	134	104	152	108	192	2.71	125	1840	3690
Cr	119	81.0	63.5	119	121	151	3.57	124	1820	4200
Co	30.1	29.9	22.2	30.1	19.1	33.1	2.42	22.4	1420	3480
Ni	51.8	39.7	31.2	51.8	47.1	62.0	3.08	49.0	1810	4290
Cu	41.3	30.0	25.8	41.3	36.4	49.5	2.89	37.6	1290	2970
Zn	80.7	78.0	73.0	80.7	34.6	49.5	1.60	35.7	1550	3310
Ga	18.1	18.0	17.7	18.1	3.66	4.32	1.23	3.69	1120	2320
Ge	-	-	-	-	-	-	-	-	0	0.0
As	2.9	1.3	1.4	2.9	4.2	2.4	3.1	3.2	200	368
Se	77.5	53.0	57.1	77.5	63.9	69.0	2.2	57.8	136	158
Br	-	-	-	-	-	-	-	-	0	0
Rb	59.1	43.8	35.1	59.1	51.8	80.0	3.16	56.5	1910	4030
Sr	245	201	201	245	151	204	1.91	149	2100	4730
Y	24.3	22.5	21.9	24.3	11.0	15.0	1.60	11.0	1970	4460
Zr	133	123	115	133	69.5	97.0	1.77	70.9	2070	4650
Nb	8.61	7.20	6.90	8.61	5.47	7.93	2.02	5.55	1790	3790
Mo	1.29	0.520	0.670	1.29	1.56	1.48	3.10	1.37	208	354
Ru	-	-	-	-	-	-	-	-	0	0
Rh	0.0	0.0	0.0	0.0	0.0	0.0	0.0	0.0	0	0
Pd	1.71	0.85	0.89	1.71	2.20	1.70	3.09	1.81	118	218
Ag	47.7	48.0	34.2	47.7	22.1	25.0	3.4	37.1	150	200
Cd	66.2	60.0	49.1	66.2	36.4	58.0	3.0	49.0	146	192
In	0.0712	0.0712	0.0712	-	0.0	0.0	1.0	-	1	28
Sn	3.08	1.60	1.85	3.08	3.58	2.75	2.67	2.90	215	377
Sb	0.30	0.20	0.21	0.30	0.27	0.32	2.38	0.25	253	497
Te	0.08	0.05	0.05	0.08	0.11	0.05	2.76	0.08	8	14
I	-	-	-	-	-	-	-	-	0	0
Cs	1.8	1.2	1.1	1.8	1.8	2.0	2.9	1.7	752	1680
Ba	399	330	268	399	306	486	2.7	337	2030	4400
La	22.3	18.1	15.8	22.3	16.7	25.5	2.5	17.5	1820	3920
Ce	44.4	36.5	33.1	44.4	31.8	46.4	2.3	32.7	1790	3870
Pr	5.6	4.7	4.3	5.6	3.8	5.4	2.1	3.9	1110	2120
Nd	21.6	18.3	17.7	21.6	13.5	18.0	1.9	13.3	1710	3500
Sm	4.6	4.1	4.0	4.6	2.4	3.0	1.7	2.3	1630	3470
Eu	1.1	1.1	1.0	1.1	0.5	0.6	1.5	0.5	1640	3470
Gd	4.4	3.9	3.9	4.4	2.1	2.7	1.6	2.1	1390	2700
Tb	0.7	0.7	0.7	0.7	0.3	0.4	1.6	0.3	1250	2860
Dy	4.3	3.9	3.8	4.3	2.0	2.8	1.6	2.0	1150	2330
Ho	0.9	0.8	0.8	0.9	0.4	0.6	1.6	0.4	1050	2100
Er	2.5	2.3	2.2	2.5	1.2	1.7	1.7	1.2	1150	2250
Tm	0.4	0.4	0.3	0.4	0.2	0.2	1.6	0.2	821	1960
Yb	2.4	2.2	2.1	2.4	1.1	1.5	1.7	1.1	1740	3740
Lu	0.4	0.3	0.3	0.4	0.2	0.2	1.7	0.2	1550	3240
Hf	3.9	3.4	3.3	3.9	2.3	3.1	1.9	2.3	1320	2830
Ta	0.7	0.5	0.5	0.7	0.5	0.7	2.3	0.5	1120	2540
W	1.0	0.4	0.5	1.0	2.0	0.8	2.9	1.1	182	454
Re	-	-	-	-	-	-	-	-	0	6
Os	-	-	-	-	-	-	-	-	0	6
Ir	0.2	0.2	0.2	0.2	0.1	0.1	1.8	0.1	6	19
Pt	1.7	0.7	0.9	1.7	2.0	1.9	3.1	1.8	120	217
Au	2.0	0.8	1.0	2.0	2.7	1.9	3.0	2.2	160	271
Hg	0.0	0.0	0.0	0.0	0.0	0.0	2.2	0.0	4	12
Tl	0.6	0.5	0.3	0.6	0.5	0.8	3.9	0.6	20	60
Pb	13.2	11.7	10.5	13.2	8.3	11.5	2.1	8.6	1260	2490
Bi	0.1	0.1	0.1	0.1	0.1	0.1	2.2	0.1	143	200
Th	5.6	3.7	3.0	5.6	5.4	8.2	3.6	5.9	1600	3330
U	1.4	1.0	0.9	1.4	1.1	1.5	2.6	1.1	1390	2700

Table S2: Granulite Facies Xenoliths

	Mean	Median	Geometric Mean	γ Mean	STD	IQR	Geo STD	γ STD	N (filtered)	N (original)
Li	11.8	6.9	9.2	11.8	10.5	6.5	1.9	8.0	12	154
Be	0.5	0.5	0.5	0.5	0.0	0.0	1.1	0.0	2	20
B	-	-	-	-	-	-	-	-	0	0
N	-	-	-	-	-	-	-	-	0	0
F	-	-	-	-	-	-	-	-	0	35
S	143	140	89.8	143.0	110.8	220.6	2.85	129.8	4	67
Cl	151.0	151.0	151.0	-	0.0	0.0	1.0	-	1	28
Sc	28.0	28.0	26.5	28.0	9.0	11.9	1.4	9.1	97	863
V	186.0	186.0	166.0	186.0	79.4	100.0	1.7	88.1	92	1030
Cr	210.0	168.0	165.0	210.0	145.0	162.0	2.1	140.0	120	1140
Co	48.9	46.8	46.5	48.9	15.1	23.5	1.4	15.5	87	759
Ni	103.0	100.0	91.6	103.0	46.7	65.0	1.7	48.3	100	1080
Cu	43.4	37.8	36.0	43.4	27.4	33.1	1.9	25.9	72	774
Zn	77.6	81.1	73.0	77.6	25.2	43.3	1.4	26.9	72	751
Ga	17.1	17.3	16.8	17.1	3.1	4.6	1.2	3.2	48	391
Ge	-	-	-	-	-	-	-	-	0	0
As	-	-	-	-	-	-	-	-	0	0
Se	-	-	-	-	-	-	-	-	0	0
Br	-	-	-	-	-	-	-	-	0	0
Rb	15.5	10.6	10.0	15.5	13.0	20.2	2.8	13.6	112	1180
Sr	482.0	465.0	437.0	482.0	207.0	315.0	1.6	210.0	121	1280
Y	19.9	19.0	17.3	19.9	9.9	16.6	1.8	10.5	102	1030
Zr	91.3	83.3	70.5	91.3	58.9	88.7	2.2	63.1	105	1060
Nb	8.8	7.0	7.0	8.8	5.8	7.7	2.0	5.8	99	888
Mo	2.3	1.9	2.1	2.3	1.2	0.8	1.6	1.1	6	62
Ru	-	-	-	-	-	-	-	-	0	0
Rh	0.0	0.0	0.0	0.0	0.0	0.0	0.0	0.0	0	0
Pd	5.54	5.54	5.54	-	0.00	0.00	1.00	-	1	5
Ag	-	-	-	-	-	-	-	-	0	0
Cd	-	-	-	-	-	-	-	-	0	0
In	-	-	-	-	-	-	-	-	0	0
Sn	1.70	1.58	1.62	1.70	0.52	0.96	1.39	0.54	9	77
Sb	-	-	-	-	-	-	-	-	0	39
Te	-	-	-	-	-	-	-	-	0	0
I	-	-	-	-	-	-	-	-	0	0
Cs	0.752	0.390	0.316	0.752	0.960	0.871	4.280	0.901	44	340
Ba	470	393	358	470	330	428	2	334	107	1120
La	14.1	11.6	11.5	14.1	8.6	12.9	2.0	8.7	118	1080
Ce	30.0	27.0	25.0	30.0	17.2	27.4	1.9	17.6	119	1090
Pr	3.6	3.5	3.0	3.6	2.1	3.3	2.0	2.2	63	535
Nd	15.8	14.7	13.7	15.8	8.0	12.3	1.8	8.4	115	1080
Sm	3.8	3.6	3.4	3.8	1.7	2.3	1.6	1.7	114	1070
Eu	1.2	1.3	1.2	1.2	0.4	0.6	1.4	0.4	108	983
Gd	3.8	3.8	3.4	3.8	1.7	2.4	1.7	1.8	79	705
Tb	0.6	0.6	0.5	0.6	0.3	0.3	1.6	0.3	93	778
Dy	3.7	3.6	3.2	3.7	1.8	3.0	1.8	2.0	73	656
Ho	0.7	0.6	0.6	0.7	0.3	0.6	1.7	0.3	63	538
Er	2.0	1.9	1.7	2.0	1.1	1.9	1.9	1.2	71	645
Tm	0.3	0.3	0.2	0.3	0.2	0.3	2.0	0.2	41	344
Yb	1.9	1.7	1.6	1.9	1.0	1.6	1.7	1.0	109	973
Lu	0.3	0.2	0.2	0.3	0.2	0.3	1.7	0.1	99	815
Hf	2.5	2.1	2.0	2.5	1.6	1.3	1.8	1.4	82	680
Ta	0.8	0.6	0.6	0.8	0.5	0.7	2.1	0.5	62	444
W	2.4	1.9	1.8	2.4	1.7	2.6	2.2	1.7	4	30
Re	-	-	-	-	-	-	-	-	0	1
Os	0.2	0.2	0.2	-	0.0	0.0	1.0	-	1	4
Ir	0.3	0.3	0.3	-	0.0	0.0	1.0	-	1	5
Pt	2.5	2.5	2.5	-	0.0	0.0	1.0	-	1	6
Au	-	-	-	-	-	-	-	-	0	3
Hg	-	-	-	-	-	-	-	-	0	0
Tl	-	-	-	-	-	-	-	-	0	0
Pb	5.6	4.5	4.6	5.6	3.6	4.9	2.0	3.5	77	690
Bi	-	-	-	-	-	-	-	-	0	0
Th	1.8	0.8	0.9	1.8	2.4	1.5	3.0	1.9	94	750
U	0.4	0.2	0.3	0.4	0.5	0.3	2.5	0.4	77	604

Table S3: Post-Archean Granulite Terrains

	Mean	Median	Geometric Mean	γ Mean	STD	IQR	Geo STD	γ STD	N (filtered)	N (original)
Li	7.9	7.2	7.3	7.9	3.2	4.7	1.5	3.1	6	74
Be	2.0	1.6	1.9	2.0	0.7	1.1	1.4	0.6	3	36
B	-	-	-	-	-	-	-	-	0	0
N	-	-	-	-	-	-	-	-	0	0
F	-	-	-	-	-	-	-	-	3	9
S	300.0	300.0	300.0	-	-	-	-	-	1	10
Cl	100.0	100.0	100.0	-	0.0	0.0	1.0	-	2	6
Sc	25.4	25.6	22.7	25.4	10.5	14.3	1.7	11.9	50	635
V	163.0	157.0	145.0	163.0	68.9	90.9	1.7	78.9	54	1030
Cr	198.0	132.0	126.0	198.0	209.0	183.0	2.6	176.0	81	1130
Co	32.3	31.8	27.8	32.3	16.5	21.6	1.8	17.2	41	677
Ni	80.4	59.0	55.7	80.4	78.4	64.8	2.3	65.5	82	1110
Cu	34.2	29.0	28.2	34.2	20.4	27.7	1.9	20.6	45	748
Zn	81.1	77.7	76.4	81.1	29.4	37.6	1.4	27.7	67	949
Ga	18.6	18.0	18.4	18.6	2.8	3.9	1.2	2.8	38	774
Ge	-	-	-	-	-	-	-	-	0	0
As	-	-	-	-	-	-	-	-	0	0
Se	-	-	-	-	-	-	-	-	0	0
Br	-	-	-	-	-	-	-	-	0	0
Rb	65.2	59.0	42.6	65.2	48.1	79.0	3.0	56.9	127	1340
Sr	280.0	267.0	240.0	280.0	144.0	190.0	1.8	152.0	134	1420
Y	28.7	24.2	24.9	28.7	15.8	17.3	1.7	14.9	67	1170
Zr	166.0	136.0	127.0	166.0	114.0	147.0	2.2	118.0	90	1330
Nb	9.9	9.5	7.7	9.9	6.2	7.9	2.3	6.9	63	948
Mo	2.4	3.2	1.8	2.4	1.3	2.1	2.3	1.7	3	37
Ru	-	-	-	-	-	-	-	-	0	0
Rh	0.0	0.0	0.0	0.0	0.0	0.0	0.0	0.0	0	0
Pd	-	-	-	-	-	-	-	-	0	0
Ag	-	-	-	-	-	-	-	-	0	0
Cd	-	-	-	-	-	-	-	-	0	0
In	-	-	-	-	-	-	-	-	0	0
Sn	3.6	2.9	3.0	3.6	2.6	2.7	1.8	2.3	5	223
Sb	0.1	0.1	0.0	0.1	0.1	0.1	2.9	0.1	6	60
Te	-	-	-	-	-	-	-	-	0	0
I	-	-	-	-	-	-	-	-	0	0
Cs	1.7	0.7	0.6	1.7	2.0	2.5	6.0	2.3	24	530
Ba	470.0	461.0	360.0	470.0	280.0	447.0	2.4	330.0	83	1260
La	26.8	24.5	20.9	26.8	16.7	24.4	2.2	18.3	63	1050
Ce	55.6	50.5	45.0	55.6	33.3	42.5	2.0	35.0	62	1060
Pr	6.0	6.1	4.3	6.0	3.9	5.4	2.7	4.7	27	588
Nd	25.9	24.8	21.6	25.9	15.3	17.1	1.9	15.1	57	878
Sm	5.2	4.9	4.5	5.2	2.8	3.0	1.8	2.8	55	842
Eu	1.3	1.4	1.2	1.3	0.4	0.7	1.4	0.4	53	836
Gd	4.9	4.4	4.3	4.9	2.6	2.3	1.7	2.4	42	683
Tb	0.9	0.7	0.8	0.9	0.5	0.5	1.8	0.5	44	759
Dy	4.3	3.7	3.9	4.3	2.0	2.4	1.6	1.9	32	634
Ho	0.9	0.8	0.8	0.9	0.4	0.6	1.6	0.4	31	607
Er	2.5	2.1	2.3	2.5	1.2	1.3	1.6	1.2	33	642
Tm	0.5	0.4	0.4	0.5	0.2	0.4	1.6	0.2	13	67
Yb	2.5	2.0	2.2	2.5	1.3	1.5	1.7	1.3	61	862
Lu	0.4	0.4	0.3	0.4	0.2	0.2	1.7	0.2	48	802
Hf	4.1	4.1	3.3	4.1	2.3	3.0	2.0	2.5	41	666
Ta	0.7	0.5	0.5	0.7	0.5	0.7	2.4	0.5	29	578
W	-	-	-	-	-	-	-	-	0	29
Re	-	-	-	-	-	-	-	-	0	0
Os	-	-	-	-	-	-	-	-	0	0
Ir	-	-	-	-	-	-	-	-	0	0
Pt	-	-	-	-	-	-	-	-	0	0
Au	-	-	-	-	-	-	-	-	0	0
Hg	-	-	-	-	-	-	-	-	0	0
Tl	-	-	-	-	-	-	-	-	0	18
Pb	13.2	11.7	10.4	13.2	8.2	12.1	2.1	8.7	35	728
Bi	-	-	-	-	-	-	-	-	0	14
Th	9.9	5.4	4.2	9.9	10.2	16.2	4.9	11.7	90	816
U	1.0	0.8	0.7	1.0	0.9	1.0	2.8	0.9	83	732

Units: Pd,W, Re, Os, Ir, Pt, and Au are in ppb. All other elements are in ppm.

Table S4: Archean Granulite Terrains

	Mean	Median	Geometric Mean	γ Mean	STD	IQR	Geo STD	γ STD	N (filtered)	N (original)
Li	15.3	16.3	14.4	15.3	4.6	7.6	1.4	5.0	4	84
Be	-	-	-	-	-	-	-	-	0	0
B	-	-	-	-	-	-	-	-	0	0
N	-	-	-	-	-	-	-	-	0	0
F	-	-	-	-	-	-	-	-	0	1
S	1772	1772.0	698	1772	2303	3260	4.9	2190	2	5
Cl	90.0	90.0	90.0	-	0.0	0.0	1.0	-	1	6
Sc	16.6	16.1	13.1	16.6	9.8	13.9	2.2	11.0	33	468
V	119.0	115.0	102.0	119.0	62.0	81.0	1.8	64.0	48	1000
Cr	146.0	117.0	104.0	146.0	108.0	170.0	2.4	114.0	67	1060
Co	41.3	35.7	33.6	41.3	25.4	38.1	1.9	25.7	35	604
Ni	72.4	55.0	54.9	72.4	52.1	76.7	2.2	51.7	69	1090
Cu	28.5	24.7	22.4	28.5	17.5	30.3	2.1	18.9	32	736
Zn	66.0	65.9	61.9	66.0	22.0	32.6	1.5	23.6	40	875
Ga	20.2	19.5	19.9	20.2	3.7	4.9	1.2	3.6	27	703
Ge	-	-	-	-	-	-	-	-	0	0
As	30.0	30.0	30.0	-	0.0	0.0	1.0	-	1	11
Se	-	-	-	-	-	-	-	-	0	6
Br	-	-	-	-	-	-	-	-	0	0
Rb	44.2	37.0	23.9	44.2	39.9	63.2	3.7	45.5	89	1340
Sr	307.0	295.0	237.0	307.0	185.0	333.0	2.2	212.0	87	1360
Y	18.4	17.8	15.8	18.4	9.4	13.0	1.8	9.9	70	1130
Zr	155.0	137.0	135.0	155.0	86.4	75.7	1.7	79.8	84	1270
Nb	9.2	7.3	7.5	9.2	6.6	5.7	1.9	5.7	66	973
Mo	-	-	-	-	-	-	-	-	0	2
Ru	-	-	-	-	-	-	-	-	0	0
Rh	0.0	0.0	0.0	0.0	0.0	0.0	0.0	0.0	0	0
Pd	-	-	-	-	-	-	-	-	0	3
Ag	-	-	-	-	-	-	-	-	0	0
Cd	-	-	-	-	-	-	-	-	0	0
In	-	-	-	-	-	-	-	-	0	0
Sn	2.6	2.5	2.5	2.6	0.7	1.2	1.4	0.8	23	95
Sb	-	-	-	-	-	-	-	-	0	6
Te	-	-	-	-	-	-	-	-	0	0
I	-	-	-	-	-	-	-	-	0	0
Cs	1.8	0.9	0.8	1.8	2.2	2.4	4.2	2.1	38	229
Ba	561.0	559.0	459.0	561.0	316.0	425.0	2.0	346.0	69	1220
La	27.3	20.0	21.8	27.3	20.6	24.5	1.9	17.6	66	993
Ce	49.8	40.0	41.6	49.8	33.8	34.5	1.8	28.9	65	987
Pr	5.0	4.4	4.4	5.0	2.6	2.7	1.7	2.4	39	376
Nd	18.1	16.4	15.8	18.1	9.2	8.6	1.7	9.3	64	594
Sm	3.6	3.3	3.3	3.6	1.5	2.3	1.5	1.5	55	661
Eu	1.1	1.1	1.1	1.1	0.3	0.5	1.4	0.33	53	641
Gd	3.5	3.3	3.2	3.5	1.5	2.2	1.6	1.56	45	455
Tb	0.5	0.5	0.5	0.5	0.2	0.3	1.6	0.22	50	571
Dy	3.3	3.0	3.0	3.3	1.2	1.9	1.5	1.28	39	481
Ho	0.6	0.6	0.6	0.6	0.3	0.4	1.7	0.30	40	417
Er	1.8	1.7	1.5	1.8	0.8	0.9	1.8	0.93	42	484
Tm	0.3	0.3	0.3	0.3	0.1	0.1	1.2	0.05	9	86
Yb	1.6	1.6	1.4	1.6	0.8	1.3	1.9	0.91	53	630
Lu	0.3	0.3	0.2	0.3	0.1	0.1	1.8	0.13	35	524
Hf	3.2	3.1	3.0	3.2	0.9	1.4	1.4	0.95	44	377
Ta	0.7	0.4	0.4	0.7	0.9	0.3	2.5	0.61	26	258
W	6.7	6.7	6.7	-	0.0	0.0	1.0	-	1	7
Re	-	-	-	-	-	-	-	-	0	0
Os	-	-	-	-	-	-	-	-	0	0
Ir	-	-	-	-	-	-	-	-	0	7
Pt	-	-	-	-	-	-	-	-	0	3
Au	-	-	-	-	-	-	-	-	0	6
Hg	-	-	-	-	-	-	-	-	0	0
Tl	-	-	-	-	-	-	-	-	0	0
Pb	10.0	8.0	8.8	10.0	5.4	5.4	1.6	4.77	61	758
Bi	-	-	-	-	-	-	-	-	0	0
Th	7.4	2.7	2.9	7.4	14.6	5.2	3.7	9.21	73	772
U	1.2	0.5	0.6	1.2	1.7	1.4	3.3	1.28	66	562

Units: Pd,W, Re, Os, Ir, Pt, and Au are in ppb. All other elements are in ppm.

Table S5: Eclogite Facies Xenoliths

	Mean	Median	Geometric Mean	γ Mean	STD	IQR	Geo STD	γ STD	N (filtered)	N (original)
Li	28.7	28.7	28.7	-	0.0	0.0	1.0	-	1	8
Be	-	-	-	-	-	-	-	-	0	0
B	-	-	-	-	-	-	-	-	0	0
N	-	-	-	-	-	-	-	-	0	0
F	-	-	-	-	-	-	-	-	0	4
S	-	-	-	-	-	-	-	-	0	0
Cl	-	-	-	-	-	-	-	-	0	4
Sc	56.2	57.0	55.6	56.2	7.5	13.8	1.15	7.6	3	33
V	320	274	314	320	62.4	120	1.21	61.0	5	60
Cr	626	764	552	626	278	554	1.70	308	5	60
Co	62.7	65.2	61.6	62.7	11.4	20.5	1.21	11.9	4	35
Ni	182	157	174	182	53.5	110	1.34	53.2	5	60
Cu	55.2	55.2	55.1	55.2	4.13	8.26	1.08	4.1	2	31
Zn	72.3	68.9	70.9	72.3	14.3	25.5	1.21	14.0	4	58
Ga	11.4	11.4	11.4	-	0.0	0.0	1.00	-	1	46
Ge	-	-	-	-	-	-	-	-	0	0
As	-	-	-	-	-	-	-	-	0	0
Se	-	-	-	-	-	-	-	-	0	0
Br	-	-	-	-	-	-	-	-	0	0
Rb	7.4	7.1	5.4	7.4	4.9	11.0	2.4	5.6	5	41
Sr	165.0	178.0	157.0	165.0	53.5	72.0	1.4	52.0	7	67
Y	19.6	20.7	19.1	19.6	4.1	7.2	1.2	4.2	7	66
Zr	40.1	41.1	34.4	40.1	20.6	29.3	1.8	21.7	6	65
Nb	10.4	6.3	5.1	10.4	9.9	19.2	3.9	11.3	6	58
Mo	-	-	-	-	-	-	-	-	0	2
Ru	-	-	-	-	-	-	-	-	0	0
Rh	-	-	-	-	-	-	-	-	0	0
Pd	-	-	-	-	-	-	-	-	0	18
Ag	-	-	-	-	-	-	-	-	0	0
Cd	-	-	-	-	-	-	-	-	0	0
In	-	-	-	-	-	-	-	-	0	0
Sn	-	-	-	-	-	-	-	-	0	2
Sb	-	-	-	-	-	-	-	-	0	2
Te	-	-	-	-	-	-	-	-	0	0
I	-	-	-	-	-	-	-	-	0	0
Cs	-	-	-	-	-	-	-	-	0	6
Ba	370.0	239.0	242.0	370.0	350.0	382.0	2.6	323.0	7	67
La	5.6	6.0	4.3	5.6	3.5	6.0	2.2	3.9	7	62
Ce	16.5	13.9	12.3	16.5	10.9	20.7	2.3	12.3	7	62
Pr	2.2	1.9	1.9	2.2	1.3	1.9	1.9	1.3	4	30
Nd	9.7	7.9	7.9	9.7	6.2	9.5	1.9	6.0	6	37
Sm	2.6	2.3	2.5	2.6	1.1	1.0	1.4	1.0	5	34
Eu	1.0	0.8	1.0	1.0	0.2	0.4	1.3	0.2	5	34
Gd	2.8	2.4	2.7	2.8	0.8	1.1	1.3	0.8	4	30
Tb	0.4	0.4	0.4	0.4	0.1	0.1	1.2	0.1	5	34
Dy	3.0	3.0	2.9	3.0	0.5	0.9	1.2	0.5	4	30
Ho	0.6	0.6	0.6	0.6	0.1	0.2	1.2	0.1	4	30
Er	1.6	1.7	1.6	1.6	0.2	0.3	1.2	0.2	4	30
Tm	0.3	0.3	0.3	0.3	0.0	0.0	1.1	0.0	2	27
Yb	2.1	1.9	2.0	2.1	0.8	1.3	1.5	0.8	5	34
Lu	0.3	0.3	0.3	0.3	0.1	0.1	1.3	0.1	4	32
Hf	1.5	1.4	1.3	1.5	0.7	1.2	1.6	0.7	4	31
Ta	0.6	0.7	0.6	0.6	0.1	0.1	1.1	0.1	3	29
W	-	-	-	-	-	-	-	-	0	0
Re	-	-	-	-	-	-	-	-	0	0
Os	-	-	-	-	-	-	-	-	0	0
Ir	-	-	-	-	-	-	-	-	0	18
Pt	-	-	-	-	-	-	-	-	0	18
Au	-	-	-	-	-	-	-	-	0	18
Hg	-	-	-	-	-	-	-	-	0	0
Tl	-	-	-	-	-	-	-	-	0	0
Pb	2.9	2.9	2.3	2.9	1.7	3.3	2.0	1.8	4	38
Bi	-	-	-	-	-	-	-	-	0	0
Th	0.4	0.3	0.4	0.4	0.2	0.3	1.7	0.2	5	55
U	0.2	0.2	0.2	0.2	0.2	0.3	1.9	0.1	4	54

Units: Pd,W, Re, Os, Ir, Pt, and Au are in ppb. All other elements are in ppm.

Table S6: Eclogite Facies Terrains

	Mean	Median	Geometric Mean	γ Mean	STD	IQR	Geo STD	γ STD	N (filtered)	N (original)
Li	-	-	-	-	-	-	-	-	0	2
Be	-	-	-	-	-	-	-	-	0	0
B	-	-	-	-	-	-	-	-	0	0
N	-	-	-	-	-	-	-	-	0	0
F	-	-	-	-	-	-	-	-	0	2
S	-	-	-	-	-	-	-	-	0	0
Cl	-	-	-	-	-	-	-	-	0	1
Sc	37.9	30.3	31.0	37.9	23.2	41.4	1.9	23.4	3	33
V	239.0	244.0	224.0	239.0	75.4	86.5	1.5	84.3	5	14
Cr	167.0	187.0	140.0	167.0	76.6	127.0	2.0	98.2	8	39
Co	38.0	38.1	36.2	38.0	11.5	13.2	1.4	11.7	7	38
Ni	83.7	86.0	77.9	83.7	27.0	35.8	1.5	31.1	8	37
Cu	26.8	17.8	21.7	26.8	18.6	26.5	1.9	17.0	6	13
Zn	108.0	105.0	106.0	108.0	19.8	36.5	1.2	19.7	4	30
Ga	20.3	19.0	19.7	20.3	5.0	9.0	1.3	4.9	3	9
Ge	-	-	-	-	-	-	-	-	0	0
As	-	-	-	-	-	-	-	-	0	23
Se	-	-	-	-	-	-	-	-	0	0
Br	-	-	-	-	-	-	-	-	0	0
Rb	7.6	4.4	5.5	7.6	6.0	10.2	2.2	5.8	3	35
Sr	207.0	183.0	165.0	207.0	118.0	208.0	2.1	134.0	9	45
Y	27.6	26.2	24.8	27.6	12.0	22.0	1.6	12.3	6	13
Zr	89.2	107.0	81.4	89.2	33.1	60.3	1.6	37.6	7	36
Nb	6.5	5.4	6.1	6.5	2.5	4.3	1.4	2.4	3	7
Mo	-	-	-	-	-	-	-	-	0	2
Ru	-	-	-	-	-	-	-	-	0	0
Rh	-	-	-	-	-	-	-	-	0	0
Pd	-	-	-	-	-	-	-	-	0	0
Ag	-	-	-	-	-	-	-	-	0	0
Cd	-	-	-	-	-	-	-	-	0	0
In	-	-	-	-	-	-	-	-	0	0
Sn	-	-	-	-	-	-	-	-	0	2
Sb	-	-	-	-	-	-	-	-	0	25
Te	-	-	-	-	-	-	-	-	0	0
I	-	-	-	-	-	-	-	-	0	0
Cs	0.1	0.1	0.1	-	0.0	0.0	1.0	-	1	26
Ba	212.0	135.0	136.0	212.0	188.0	319.0	2.7	189.0	9	39
La	7.9	6.4	6.3	7.9	5.3	9.4	2.0	5.2	4	35
Ce	15.6	14.8	12.9	15.6	8.8	16.9	1.9	9.3	4	35
Pr	0.8	0.8	0.8	-	0.0	0.0	1.0	-	1	4
Nd	6.7	5.8	6.3	6.7	2.5	3.5	1.4	2.3	4	36
Sm	2.5	2.0	2.4	2.5	1.0	1.4	1.4	0.9	4	36
Eu	1.0	1.0	1.0	1.0	0.1	0.1	1.1	0.1	3	34
Gd	5.0	5.0	5.0	5.0	0.2	0.5	1.1	0.2	2	8
Tb	0.7	0.8	0.7	0.7	0.2	0.4	1.4	0.2	3	34
Dy	6.3	6.3	6.3	-	0.0	0.0	1.0	-	1	4
Ho	1.3	1.3	1.3	1.3	0.1	0.1	1.0	0.1	2	8
Er	3.8	3.8	3.8	3.8	0.2	0.3	1.0	0.2	2	8
Tm	0.5	0.5	0.5	-	0.0	0.0	1.0	-	1	6
Yb	3.4	3.8	3.0	3.4	1.5	2.5	1.7	1.6	6	40
Lu	0.2	0.2	0.2	-	0.0	0.0	1.0	-	1	31
Hf	1.8	1.8	1.8	-	0.0	0.0	1.0	-	1	32
Ta	0.1	0.1	0.1	-	0.0	0.0	1.0	-	1	29
W	-	-	-	-	-	-	-	-	0	0
Re	-	-	-	-	-	-	-	-	0	0
Os	-	-	-	-	-	-	-	-	0	0
Ir	-	-	-	-	-	-	-	-	0	0
Pt	-	-	-	-	-	-	-	-	0	0
Au	-	-	-	-	-	-	-	-	0	0
Hg	-	-	-	-	-	-	-	-	0	0
Tl	-	-	-	-	-	-	-	-	0	0
Pb	2.3	2.3	2.2	2.3	0.7	1.4	1.4	0.7	2	8
Bi	-	-	-	-	-	-	-	-	0	0
Th	0.2	0.2	0.2	0.2	0.1	0.3	2.1	0.1	2	32
U	0.1	0.1	0.1	-	0.0	0.0	1.0	-	1	32

Units: Pd,W, Re, Os, Ir, Pt, and Au are in ppb. All other elements are in ppm.

Table S7. Amphibolite Facies Lithologies

	Mean	Median	Geo Mean	γ Mean	STD	IQR	Geo STD	γ STD	N(filtered)	N(original)
La/Yb	11.6	8.16	7.15	11.6	10.9	13.40	2.88	10.7	1740	3740
Nb/Ta	14.4	14.1	12.6	14.4	5.99	6.33	1.99	7.37	719	1360
Zr/Hf	35.5	35.6	35.0	35.5	6.08	7.70	1.20	6.27	1320	2820
Rb/Cs	48.5	34.0	31.4	48.5	45.4	41.90	2.80	42.7	753	1580
K/Rb	331	294	299	331	160	183.00	1.56	147	1900	3960
La/Th	6.62	5.02	5.30	6.62	4.75	5.42	1.93	4.27	1590	3200
Th/U	4.20	3.65	3.35	4.20	2.67	3.10	2.08	2.73	1380	2600
K/U	15900	12100	11300	15900	13000	14200.00	2.42	12600	1380	2600
Eu/Eu*	0.859	0.884	0.826	0.859	0.229	0.32	1.34	0.241	1372	2674
κ_{Pb}	3.89	3.86	3.84	3.89	0.646	0.48	1.17	0.621	-	165
Heat Prod. (nW/kg)	0.470	0.278	0.240	0.470	1.99	0.46	3.16	0.503	490	1467
Heat Prod. (mW/m^3)	1.36	0.81	0.70	1.36						

Table S8. Granulite Facies Xenoliths

	Mean	Median	Geo Mean	γ Mean	STD	IQR	Geo STD	γ STD	N(filtered)	N(original)
La/Yb	8.71	7.52	7.29	8.71	5.33	6.37	1.83	5.05	103	957
Nb/Ta	18.0	18.6	15.3	18	7.54	9.1	2.14	9.98	41	424
Zr/Hf	39.9	36.3	36.4	39.9	17.8	11.5	1.56	16.9	62	669
Rb/Cs	73.4	40.6	37.2	73.4	84.1	52	3.83	79	39	317
K/Rb	788	643	653	788	491	685	1.86	470	104	1140
La/Th	27.0	17.1	18.0	27.0	25.0	25.8	2.51	23.0	89	683
Th/U	3.79	3.39	3.05	3.79	2.47	2.67	2.03	2.42	67	571
K/U	46300	36900	32300	46300	36100	43000	2.66	37400	72	571
Eu/Eu*	1.28	1.09	1.21	1.28	0.479	0.38	1.38	0.425	79	703
κ_{Pb}	4.17	4.04	4.14	4.17	0.520	0.24	1.11	0.464	-	357
Heat Prod.	0.147	0.0716	0.0861	0.147	0.187	0.11	2.68	0.142	62	79
Heat Prod. (mW/m^3)	0.43	0.21	0.25	0.43						

Table S9. Post Archean Granulite Facies Terrains

	Mean	Median	Geo Mean	γ Mean	STD	IQR	Geo STD	γ STD	N(filtered)	N(original)
La/Yb	11.7	10.1	8.54	11.7	7.75	8.96	2.77	8.84	41	658
Nb/Ta	14.7	13.9	9.46	14.7	10.4	8.57	4.00	13.0	22	416
Zr/Hf	35.9	35.7	35.1	35.9	7.2	11	1.24	7.46	29	479
Rb/Cs	100	44.6	44.8	100	159	81.4	3.50	116	18	386
K/Rb	423	291	346	423	335	265	1.78	259	109	1090
La/Th	23.7	11.2	12.3	23.7	30.2	18	3.05	25.0	36	777
Th/U	10.1	6.58	6.50	10.1	9.91	10	2.61	8.90	73	564
K/U	37500	31000	27500	37500	32900	32200	2.22	28300	73	564
Eu/Eu*	1.02	1.03	0.94	1.02	0.411	0.46	1.48	0.395	40	673
κ_{Pb}	3.99	4.00	3.99	3.99	0.159	0.19	1.04	0.158	-	33
Heat Prod.	0.514	0.407	0.267	0.514	0.490	0.62	4.41	0.544	70	91
Heat Prod. (mW/m^3)	1.49	1.18	0.77	1.49						

Table S10. Archean Granulite Facies Terrains

	Mean	Median	Geo Mean	γ Mean	STD	IQR	Geo STD	γ STD	N(filtered)	N(original)
La/Yb	25.4	16	18.2	25.4	20.3	31.1	2.33	19.8	45	572
Nb/Ta	17.5	16.3	16.4	17.5	6.24	6.92	1.45	6.26	16	218
Zr/Hf	35.4	35.8	34.7	35.4	7.21	9.54	1.22	7.00	39	341
Rb/Cs	86.0	61.0	44.7	86.0	94.0	93.7	3.61	90.9	30	196
K/Rb	640	433	506	640	477	515	1.95	424	81	1250
La/Th	13.4	7.32	7.8	13.4	16.1	14.2	2.88	13.1	47	728
Th/U	9.17	7.26	6.58	9.17	7.00	9.37	2.39	7.13	60	527
K/U	38100	29300	22900	38100	31900	44900	3.30	36100	60	527
Eu/Eu*	1.16	1.09	1.11	1.16	0.331	0.46	1.34	0.330	44	451
κ_{Pb}	4.16	4.11	4.16	4.16	0.164	0.23	1.03	0.141	-	4
Heat Prod.	0.558	0.179	0.207	0.558	1.04	0.36	3.73	0.708	54	70
Heat Prod. (mW/m^3)	1.62	0.52	0.60	1.62						

Table S11. Eclogite Facies Xenoliths

	Mean	Median	Geo Mean	γ Mean	STD	IQR	Geo STD	γ STD	N(filtered)	N(original)
La/Yb	6.53	4.69	4.87	6.53	5.16	7.37	2.14	4.8	7	34
Nb/Ta	16.70	17.5	7.89	16.7	10.1	16	6.43	18.8	5	29
Zr/Hf	30.20	31.7	28.4	30.2	9.24	13.5	1.47	10.6	5	31
Rb/Cs	26.60	26.6	18.5	26.6	19.1	38.3	2.48	21.6	2	6
K/Rb	542	503	458	542	287	476	1.85	306	7	41
La/Th	9.22	9.56	8.77	9.22	2.66	4.61	1.4	2.91	6	31
Th/U	2.18	2.17	2.03	2.18	0.798	1.47	1.45	0.798	5	29
K/U	16100	5190	7040	16100	17400	25600	4.29	18800	5	29
Eu/Eu*	1.01	0.968	1.01	1.01	0.095	0.14	1.09	0.0926	4	30
κ_{Pb}	5.48	5.75	5.44	5.48	0.668	1.01	1.13	0.668	-	21
Heat Prod.	0.0792	0.0433	0.0585	0.0792	0.0771	0.07	2.08	0.0590	3	5
Heat Prod. (mW/m^3)	0.23	0.13	0.17	0.23						

Table S12. Eclogite Facies Terrains

	Mean	Median	Geo Mean	γ Mean	STD	IQR	Geo STD	γ STD	N(filtered)	N(original)
La/Yb	7.46	5.48	3.96	7.46	6.9	10.4	3.69	7.77	5	40
Nb/Ta	29.40	29.4	29.4	-	0	0	1	-	1	25
Zr/Hf	27.20	27.2	20.6	27.2	17.7	35.4	2.18	19.4	2	32
Rb/Cs	53.30	53.3	52.7	53.3	7.52	15	1.15	7.55	2	23
K/Rb	693	526	564	693	498	435	1.84	431	5	35
La/Th	60.50	60.5	31.7	60.5	51.5	103	3.53	63.6	2	19
Th/U	2.73	2.56	2.7	2.73	0.424	0.746	1.16	0.415	3	26
K/U	68000	44300	24700	68000	65600	117000	6.04	87100	3	26
Eu/Eu*	0.875	0.875	0.875	0.875	0.0182	0.036	1.02	0.0182	2	8
κ_{Pb}	-	-	-	-	-	-	-	-	-	0
Heat Prod.	0.0647	0.0437	0.0539	0.0647	0.0489	0.0681	1.81	0.0380	1	3
Heat Prod. (mW/m^3)	0.19	0.13	0.16	0.19						

5. Supplementary Figures

References

Arndt, N. (1994). Archean komatiites. *Archean crustal evolution*, *10*, 11–44.

Banks, D., Green, R., Cliff, R., & Yardley, B. (2000). Chlorine isotopes in fluid inclusions: determination of the origins of salinity in magmatic fluids. *Geochimica et Cosmochimica Acta*, *64*(10), 1785–1789.

Barnes, S.-J. (2016). Chalcophile elements.

Barnhart, K. R., Mahan, K. H., Blackburn, T. J., Bowring, S. A., & Dudas, F. O. (2012). Deep crustal xenoliths from central montana, usa: Implications for the timing and mechanisms of high-velocity lower crust formation. *Geosphere*, *8*(6), 1408–1428.

Bohlen, S., & Mezger, K. (1989). Origin of granulite terranes and the formation of the lowermost continental crust. *Science*, *244*(4902), 326–329.

Field, D., & Clough, P. W. (1976). K/rb ratios and metasomatism in metabasites from a precambrian amphibolite–granulite transition zone. *Journal of the Geological Society*, *132*(3), 277–288.

Field, D., & Elliott, R. (1974). The chemistry of gabbro/amphibolite transitions in south norway. *Contributions to Mineralogy and Petrology*, *47*(1), 63–76.

Fowler, M. (1986). Large-ion lithophile element characteristics of an amphibolite facies to granulite facies transition at gruinard bay, north-west scotland. *Journal of Metamorphic Geology*, *4*(3), 345–359.

Greaney, A. T., Rudnick, R. L., Gaschnig, R. M., Whalen, J. B., Luais, B., & Clemens, J. D. (2018). Geochemistry of molybdenum in the continental crust. *Geochimica et Cosmochimica Acta*, *238*, 36–54.

Hartigan, J. A., & Hartigan, P. M. (1985). The dip test of unimodality. *The annals of*

Statistics, *13*(1), 70–84.

Jenner, F. E. (2017). Cumulate causes for the low contents of sulfide-loving elements in the continental crust. *Nature Geoscience*, *10*(7), 524–529.

Kusebauch, C., John, T., Barnes, J. D., Klügel, A., & Austrheim, H. O. (2015). Halogen element and stable chlorine isotope fractionation caused by fluid–rock interaction (bamble sector, se norway). *Journal of Petrology*, *56*(2), 299–324.

Markl, G., Musashi, M., & Bucher, K. (1997). Chlorine stable isotope composition of granulites from lofoten, norway: Implications for the cl isotopic composition and for the source of cl enrichment in the lower crust. *Earth and Planetary Science Letters*, *150*(1-2), 95–102.

Polat, A., Hofmann, A., & Rosing, M. T. (2002). Boninite-like volcanic rocks in the 3.7–3.8 ga isua greenstone belt, west greenland: geochemical evidence for intra-oceanic subduction zone processes in the early earth. *Chemical geology*, *184*(3-4), 231–254.

Rudnick, R. L., Barth, M., Horn, I., & McDonough, W. F. (2000). Rutile-bearing refractory eclogites: missing link between continents and depleted mantle. *Science*, *287*(5451), 278–281.

Rudnick, R. L., & Gao, S. (2014). Composition of the Continental Crust. In *Treatise on Geochemistry* (p. 1-51). Elsevier. doi: 10.1016/B978-0-08-095975-7.00301-6

Rudnick, R. L., & Jackson, I. (1995). Measured and calculated elastic wave speeds in partially equilibrated mafic granulite xenoliths: Implications for the properties of an underplated lower continental crust. *Journal of Geophysical Research: Solid Earth*, *100*(B6), 10211–10218.

Rudnick, R. L., McLennan, S. M., & Taylor, S. R. (1985). Large ion lithophile elements

in rocks from high-pressure granulite facies terrains. *Geochimica et Cosmochimica Acta*, *49*(7), 1645–1655.

Rudnick, R. L., & Presper, T. (1990). Geochemistry of intermediate/-to high-pressure granulites. In *Granulites and crustal evolution* (pp. 523–550). Springer.

Rudnick, R. L., & Taylor, S. R. (1987, December). The composition and petrogenesis of the lower crust: A xenolith study. *Journal of Geophysical Research: Solid Earth*, *92*(B13), 13981-14005. doi: 10.1029/JB092iB13p13981

Sighinolfi, G. P. (1971). Investigations into deep crustal levels: fractionating effects and geochemical trends related to high-grade metamorphism. *Geochimica et Cosmochimica Acta*, *35*(10), 1005–1021.

Stosch, H.-G., Lugmair, G., & Seck, H. (1986). Geochemistry of granulite-facies lower crustal xenoliths: implications for the geological history of the lower continental crust below the eifel, west germany. *Geological Society, London, Special Publications*, *24*(1), 309–317.

Tang, M., McDonough, W. F., & Ash, R. D. (2017). Europium and strontium anomalies in the morb source mantle. *Geochimica et Cosmochimica Acta*, *197*, 132–141.

Taylor, S. R., & McLennan, S. M. (1985). *The continental crust: its composition and evolution*. Blackwell Scientific Pub., Palo Alto, CA.

Van Calsteren, P., Harris, N., Hawkesworth, C., Menzies, M., & Rogers, N. (1986). Xenoliths from southern africa: a perspective on the lower crust. *Geological Society, London, Special Publications*, *24*(1), 351–362.

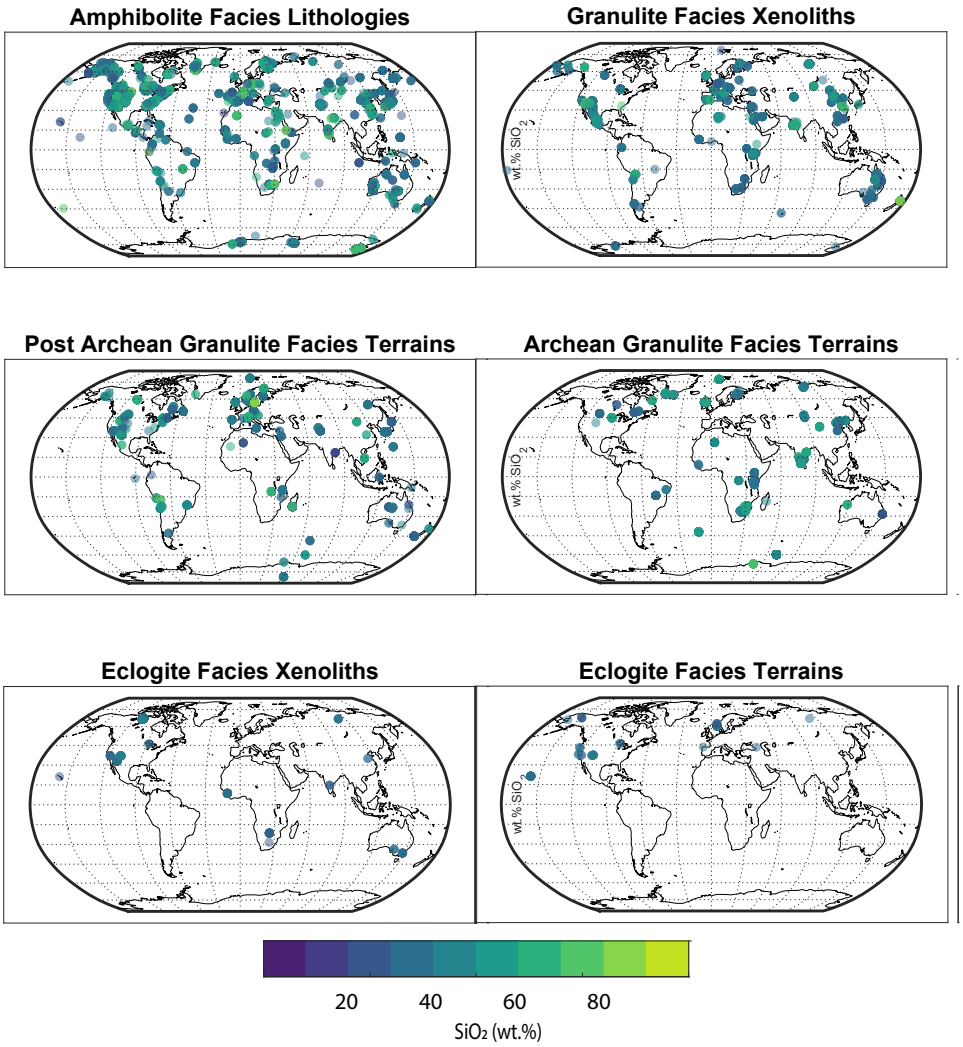

Figure S1. Maps of the metamorphic sample datasets that we have extensive sample coverage for amphibolite and granulite facies lithologies with more limited exposures of eclogite facies lithologies. Each circle is a single sample whose color is determined by weight percent SiO_2. Many circles overlap. There is little correlation between SiO_2 and location.

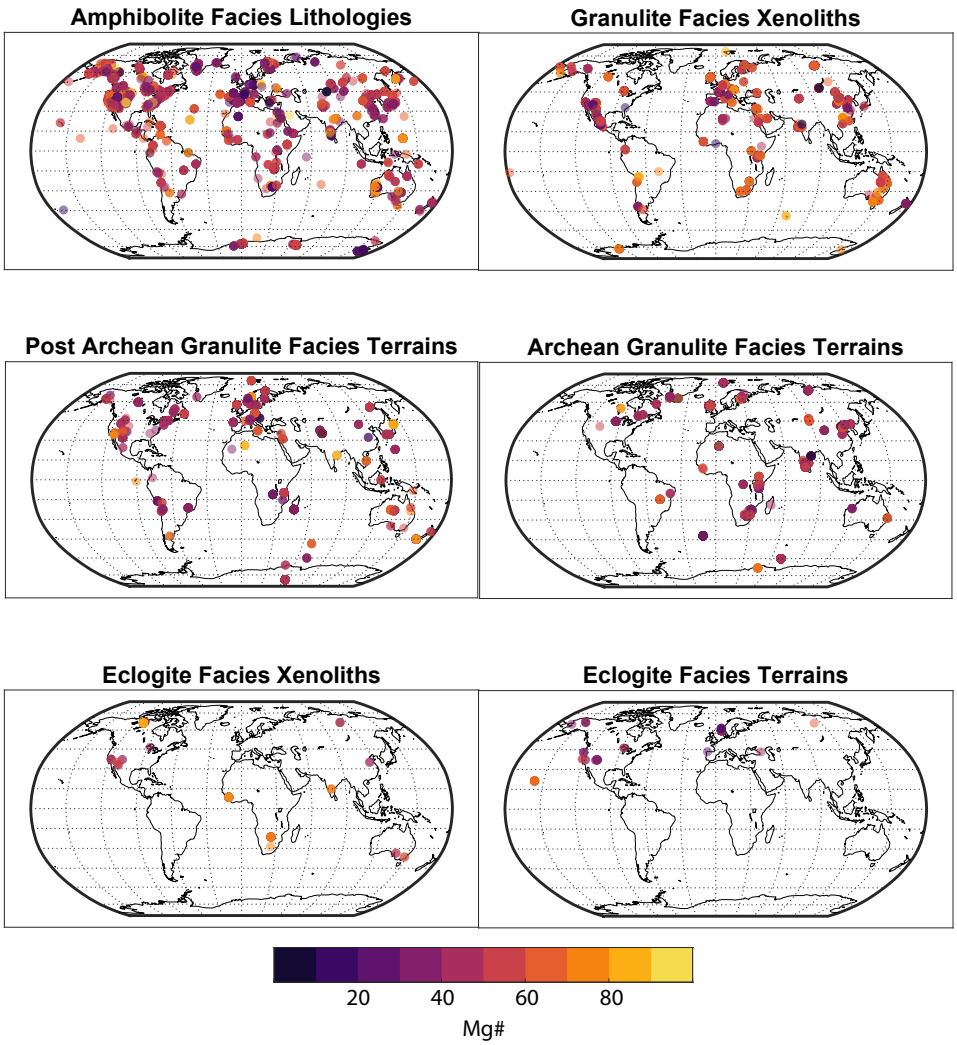

Figure S2. Maps of the metamorphic sample datasets that we have extensive sample coverage for amphibolite and granulite facies lithologies with more limited exposures of eclogite facies lithologies. Each circle is a single sample whose color is determined by weight percent SiO_2. Many circles overlap. There is no correlation between Mg# and location.

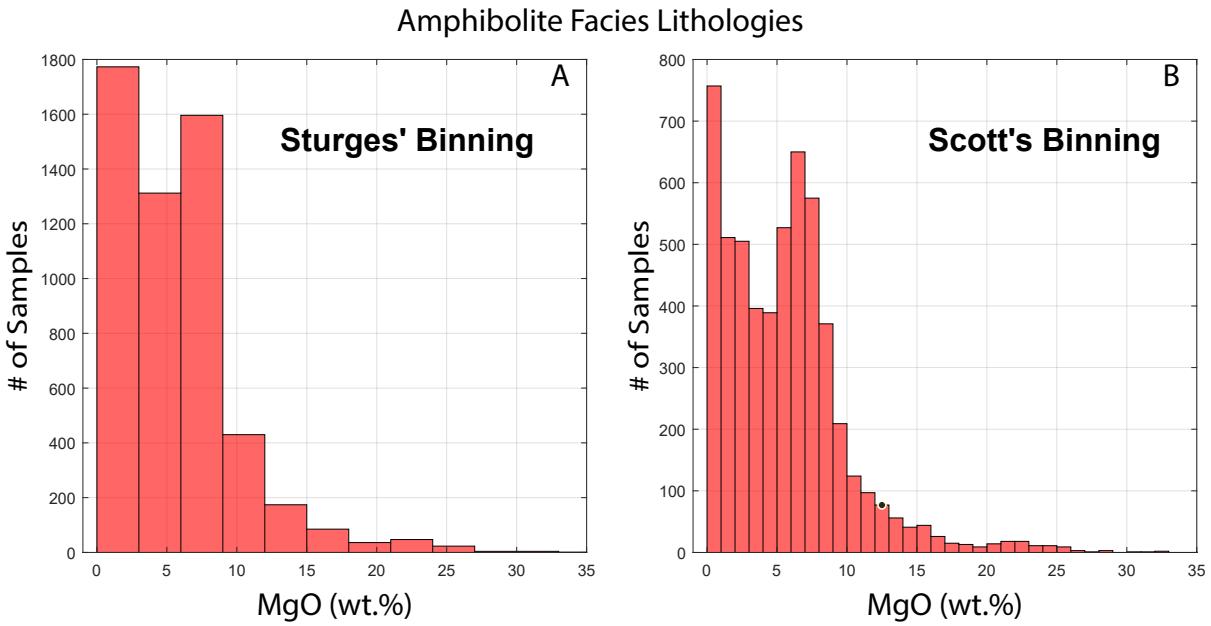

Figure S3. Amphibolite facies lithologies, when binned according to MgO, do not show obvious bimodality when binned according to Sturge's Law (fewer bins) but do show dual peaks when plotted with more bins. Such a phenomenon highlights the importance of binning and data visualization and need for more objective distribution rankings, such as the Hartigan's Dip Test.

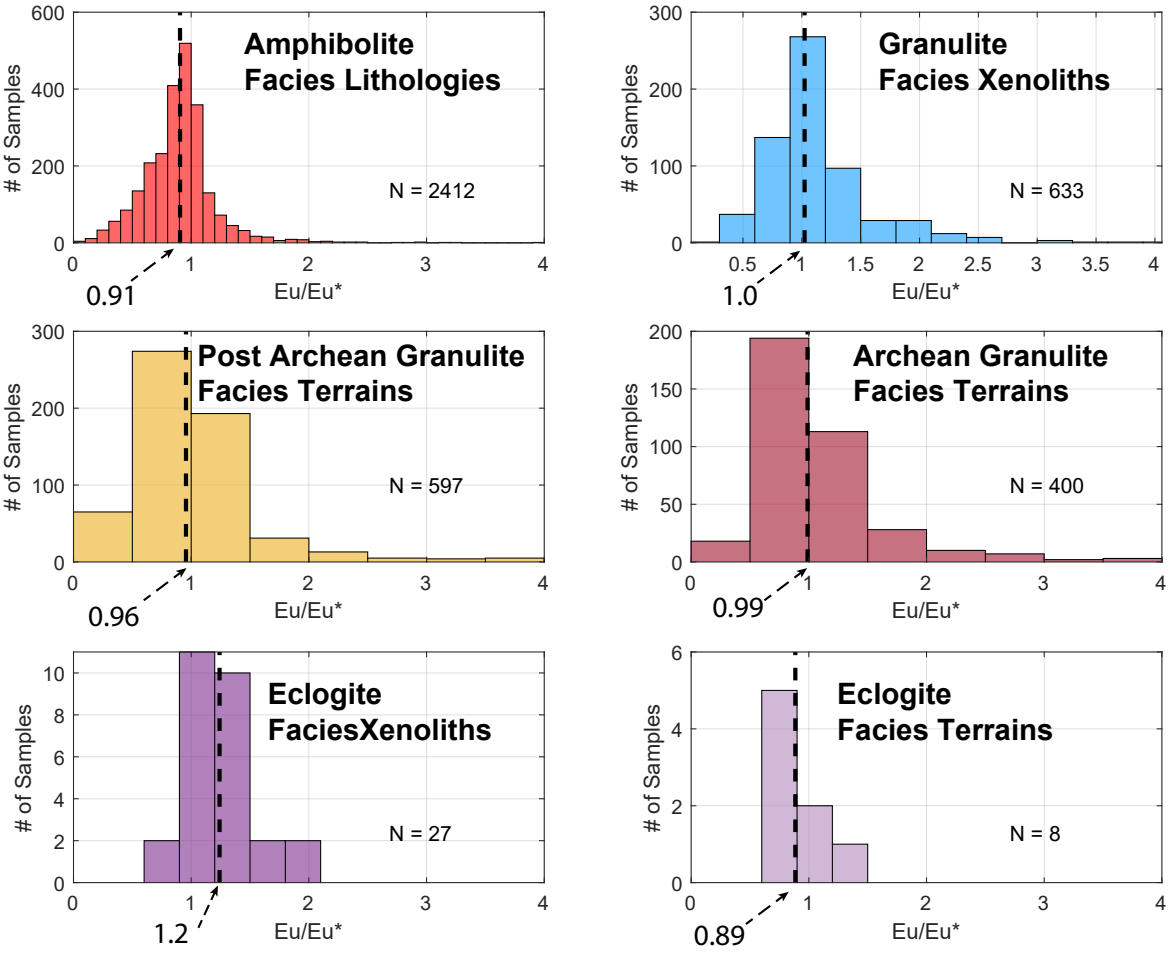

Figure S4. The right-skewed Eu/Eu* distributions of our datasets all find a median value close to 1, which is 15 - 30% less than previous estimates. Because of the asymmetry in the distributions, both granulite facies xenoliths and terrains have similar values, though the more felsic Archean granulite facies lithologies have a higher percentage of Eu/Eu* values >1 than their more mafic Post Archean counterparts.

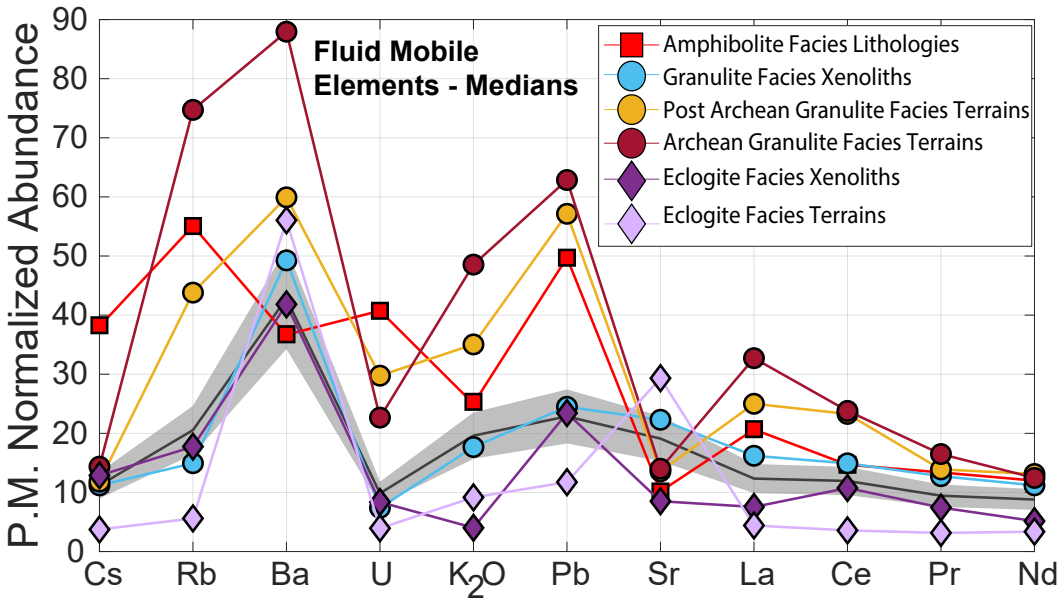

Figure S5. Fluid mobile element concentrations from amphibolite and granulite facies lithologies are comparable with previous estimates for the lower crust. Eclogite facies lithologies are up a half an order of magnitude more depleted. Variable labile element depletions cause the amphibolite facies lithologies to overlap with the granulite facies terrains, suggesting that either the amphibolite facies samples have experienced some fluid depletion or that the behavior of the labile elements is caused by an igneous process and not metamorphic dehydration. The black line and gray shaded region surrounding it is the Rudnick and Gao (2014) lower crustal composition ± 15%.

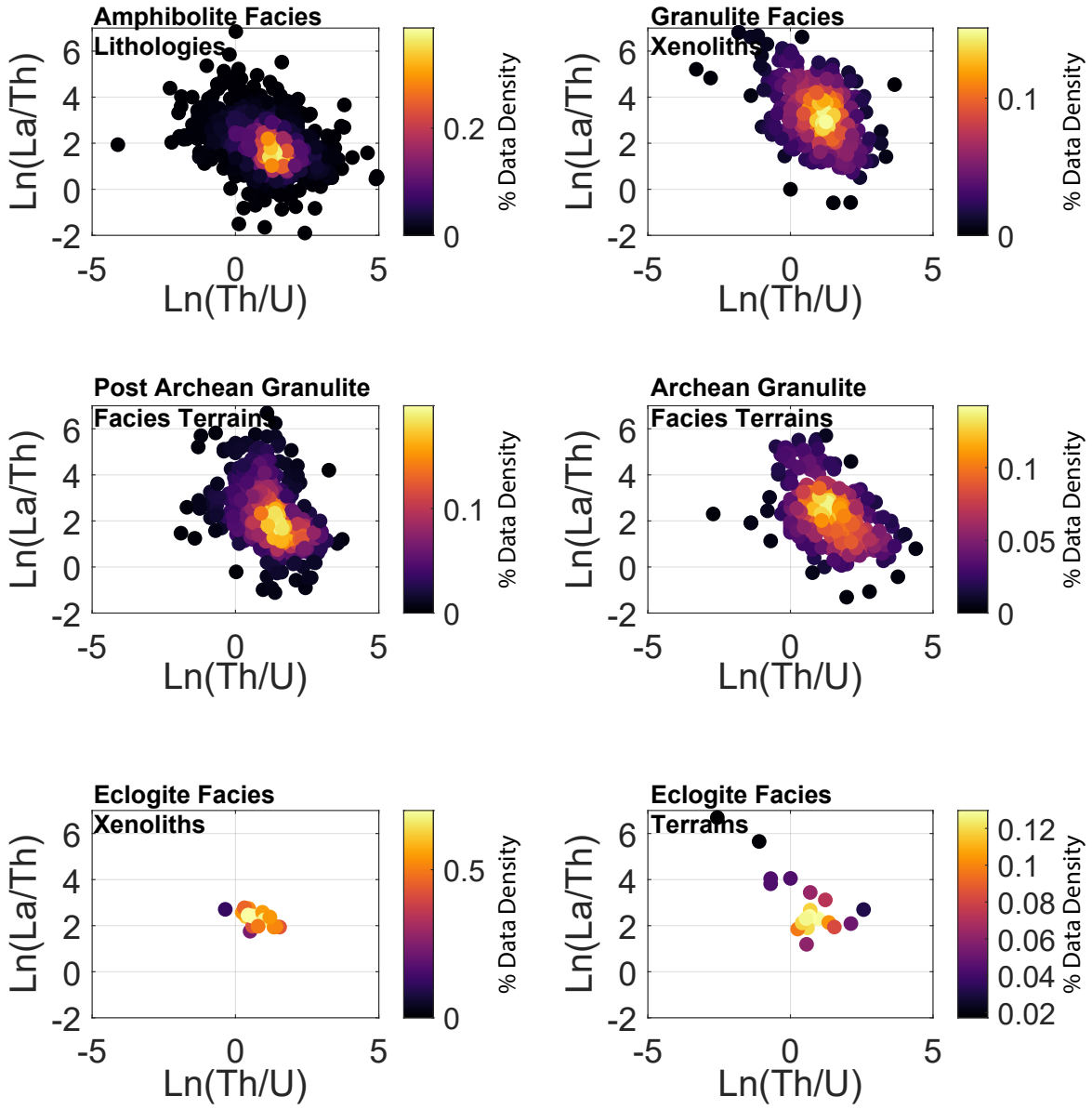

Figure S6. La/Th vs. Th/U in natural log space. Color indicates the data point density. High La/Th values correlate with low Th/U concentrations, indicating that low La/Th is due to depletions in Th instead of enrichments in La.

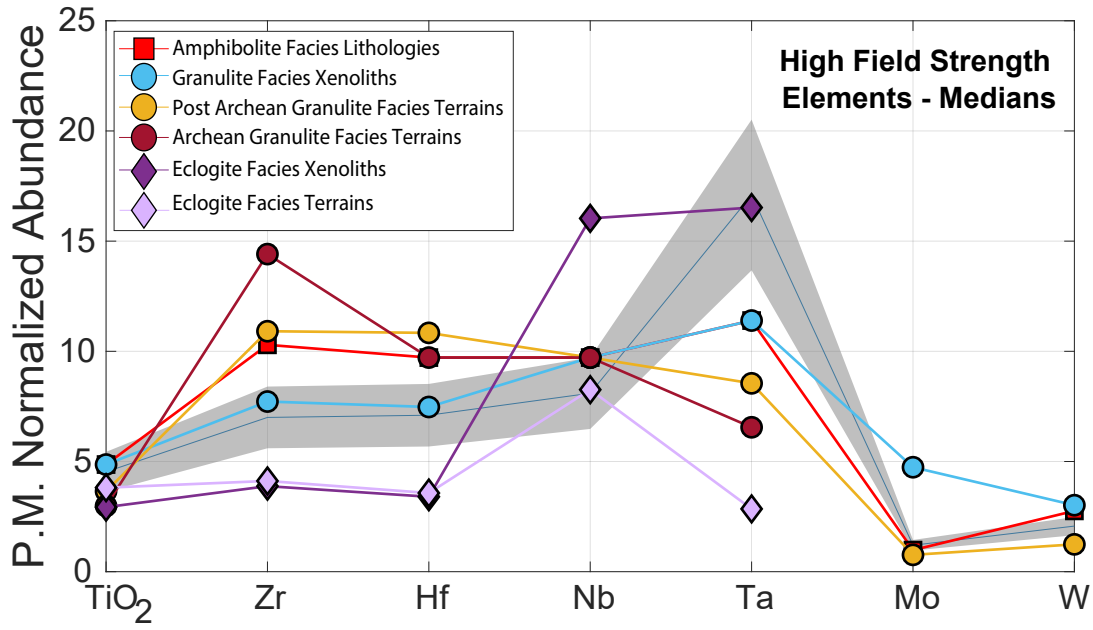

Figure S7. As with the fluid mobile elements, the high field strength element concentrations are broadly in agreement with previous estimates. Granulite facies xenoliths and eclogite facies lithologies show elevated concentrations of Mo, partly due to lack of data but also potentially because of the abundance of rutile, titanite, ilmenite, and magnetite in these predominantly mafic samples. Eclogite facies lithologies have negative Ta spikes, which are also potentially caused by the presence of rutile. The black line and gray shaded region surrounding it is the Rudnick and Gao (2014) lower crustal composition ± 15%.

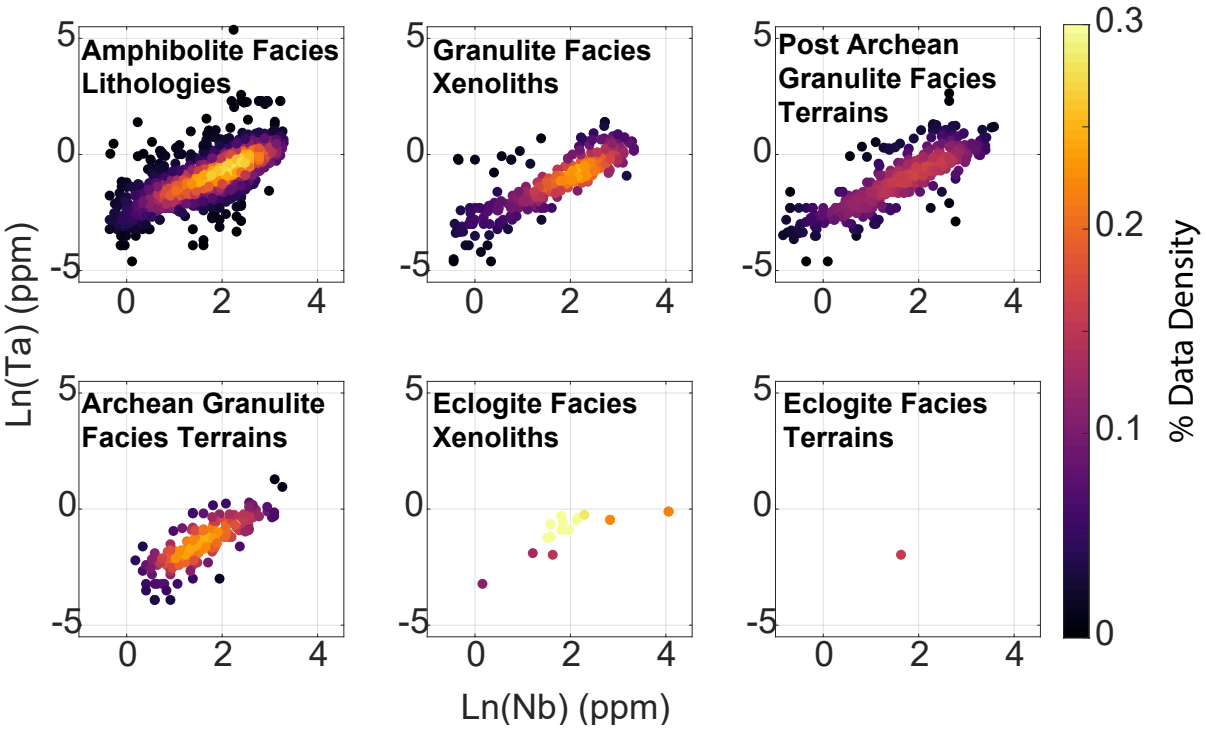

Figure S8. Nb vs. Ta forms a log-linear relationship with consistent Nb/Ta values for amphibolite and granulite facies lithologies. Color is relative data point density.

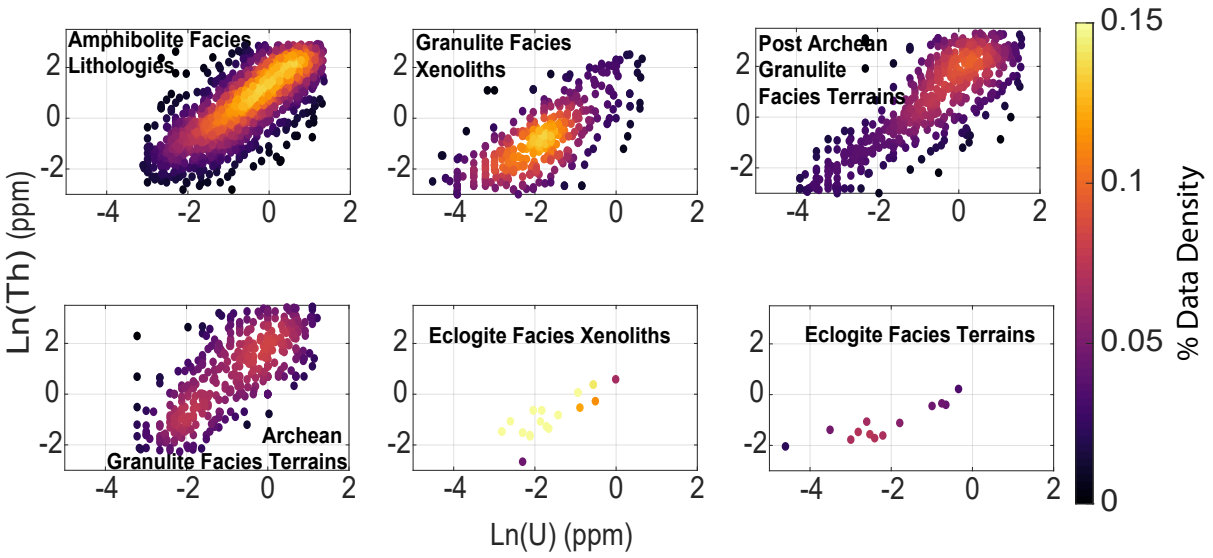

Figure S9. Ln[Th] vs. Ln[U] for amphibolite and granulite facies lithologies forms a linear trend. Color indicates relative data point density. The Th/U ratio for all lithologies forms a linear trend in log-log space. Scatter in U concentration could be caused by U's mobility in certain oxidation states since amphibolites can contain hydrous minerals.